Article

Molecular Docking *in silico* Analysis of Brazilian Essential Oils Against Host Targets and SARS-CoV-2 Proteins

Rêmullo B. G. M. Costa,[a] *Regildo M. G. Martins,[b]* *Gerlane S. de Lima,[c]*
Thayza C. M. Stamford,[d] *Wanderli P. Tadei,[†,e]* *Maria Aparecida M. Maciel,*[*,a]*
Amália C. M. do Rêgo[a] and Francisco H. Xavier-Júnior[a,f]

*[a]Programa de Pós-Graduação em Biotecnologia, Universidade Potiguar (UnP),
Campus Salgado Filho, 59075-000 Natal-RN, Brazil*

*[b]Programa Multi-Institucional de Pós-Graduação em Biotecnologia (PPGBIOTEC),
Universidade Federal do Amazonas (UFAM), 69077-000 Manaus-AM, Brazil*

[c]Departamento de Nutrição, Universidade Federal de Pernambuco (UFPE), 50670-901 Recife-PE, Brazil

[d]Departamento de Medicina Tropical, Universidade Federal de Pernambuco (UFPE), 50670-901 Recife-PE, Brazil

[e]Laboratório de Malária e Dengue, Instituto Nacional de Pesquisas Amazônicas (INPA), 69060-001 Manaus-AM, Brazil

*[f]Laboratório de Biotecnologia Farmacêutica, Universidade Federal da Paraíba (UFPB),
58051-900 João Pessoa-PB, Brazil*

The inhibitory activity of thirty-one sesquiterpenes identified from Brazilian essential oils (*Copaifera langsdorffii* Desf., *Croton cajucara* Benth. and *Siparuna guianensis* Aublet.) were analyzed by *in silico* molecular docking. The compounds were characterized by gas chromatography-mass spectrometry (GC-MS) and gas chromatography with flame-ionization detection (GC-FID), and then, applied against severe acute respiratory syndrome coronavirus-2 (SARS-CoV-2) proteins and human angiotensin-converting enzyme 2 (hACE2). Applying molecular docking and AutoDock Vina software, a total of 496 individual interactions were detected for sesquiterpenes along with SARS-CoV-2 proteins and hACE2 human angiotensin converting enzyme-2 protein. The findings showed considerable binding affinity of sesquiterpenes with the tested macromolecules. In that, β-selinene from *C. langsdorffii* displayed the best energy (-7.2 kcal mol^{-1}) and showed strong interactions with the amino acids of the SARS-CoV-2 M-Pro protein. Spathulenol from *C. cajucara* strongly interacted with human ACE2, with a binding energy of -7.1 kcal mol^{-1}. Meanwhile, γ-eudesmol from *S. guianensis* presented the lowest binding energy (-7.5 kcal mol^{-1}) by interacting with the SARS-CoV-2 M-Pro complex. Additionally, measurements were performed aiming to evaluate the best sesquiterpenes binding interactions with the main proteins and its homologue files. According to results, these Brazilian essential oils hold antiviral potential being a rich source for further *in vitro* and *in vivo* studies focusing on herbal therapeutic adjuvants against SARS-CoV-2 infections.

Keywords: SARS-CoV-2 infection, molecular docking, *Copaifera langsdorffii* Desf., *Croton cajucara* Benth., *Siparuna guianensis* Aublet., sesquiterpenes essential oils

Introduction

Severe acute respiratory syndrome coronavirus-2 (SARS-CoV-2) type has been spreading throughout the world since the end of 2019, when the first infections

were reported from China.[1,2] By mid-December of 2021, the World Health Organization reported over 271 million infected people worldwide and about 5.31 million deaths due to the complications of the COVID-19 (coronavirus disease 2019) infection.[3] SARS-CoV-2 is a virus from the Coronaviridae family, belonging to the β-coronaviruses lineage B, and represents one of the seven coronaviruses able to infect humans.[2] It is a single-stranded ribonucleic acid (RNA) genome virus, encapsulated by a membrane

envelope encrusted with transmembrane spike glycoproteins (S proteins), granting its crown-like morphology.[4]

Several studies have tried to identify SARS-CoV-2 fusion inhibitors that could mediate the membrane-fusion process associated with the human angiotensin-converting enzyme 2 (hACE2), an exopeptidase expressed on epithelial cells present in most tissues, such as lungs, kidneys, and heart, acting as the primary receptor in human cell infection.[2,4,5] Other virus proteins associated with this infection are SARS-CoV-2 M-Pro, SARS-CoV-2 Nsp15/NendoU, SARS-CoV-2 RdRP, and SARS-CoV-2 Spike S, which are responsible for the viral genome replication and generate new viruses inside host cells.[1,4,6] SARS-CoV-2 presents higher receptor-binding capacity rather than SARS-CoV, contributing to its effective transmissibility and infectivity.[4,7] Therefore, to search the effectiveness of fusion inhibitor compounds against this severe public-health threat become mandatory in the pharmacological science field. Since many herbals show antiviral activity, the phytochemicals effectiveness against SARS-CoV-2 has become of crucial interest.[6,8]

Brazil hosts 15 to 20% of the world's biological diversity, with a vast potential to discover new biocompounds from natural sources.[9] Many of the herbal extracts exhibit biological properties due to their complex mixture of compounds produced for plant protection,[10] such as flavonoids,[11] resveratrol,[12] betulinic acid, indigo, aloe-emodin, luteolin, and quinone-methide triterpenoids.[13] These compounds act as immunomodulators, suppressing inflammatory reactions, which are important aspects related to the elevated morbidity and mortality of the SARS-CoV-2 infection.[4] From this perspective, the ethanol extract of *Torreya nucifera* and its isolated diterpenoids and flavonoids exhibited good SARS-CoV 3CL(pro) inhibitory activity[13] and essential oils also presented potential against SARS-CoV-2 proteins, such as garlic oil (*Allium sativum* L.).[5]

Focusing on new findings, the essential oil of copaiba (*Copaifera langsdorffii* Desf.) has already demonstrated antibacterial, antifungal, anti-inflammatory, anti-leishmania, and anti-cancer activities[10] which have been linked to the bioactive action of non-polar diterpenes and sesquiterpenes.[10] Meanwhile, sacaca (*Croton cajucara* Benth.)[14] and negramina (*Siparuna guianensis* Aublet.)[15,16] essential oils present bioactive mono- and sesquiterpenes. To the best of our knowledge, there are no theoretical or experimental studies by assaying these essential oils against SARS-CoV-2. So, in the current study molecular docking *in silico* analysis were applied on protein-ligand interaction models, analyzing target protein groups such as: angiotensin-converting enzyme (hACE2), coronavirus main proteinase (SARS-CoV-2 MPro), SARS-CoV-2 endoribonuclease (SARS-CoV-2 Nsp15/NendoU), RNA-dependent RNA polymerase (SARS-CoV-2 RdRP), and Spike S protein. In addition, the potential application of these essential oils as adjuvants against SARS-CoV-2 are herein discussed for further *in vitro* and *in vivo* studies.

Experimental

Herbal and essential oils extraction

Samples of *Copaifera langsdorffii* Desf. (oil resin), *Croton cajucara* Benth. (leaves), and *Siparuna guianensis* Aublet. (leaves), were collected in the Tupé Sustainable Development Reserve ("*Reserva de Desenvolvimento Sustentável do Tupé- RDS Tupé*") at the Comunidade Colônia Central, located about 25 km from the city of Manaus, Amazonas state, Brazil. The essential oils were obtained by hydrodistillation in a Clevenger apparatus at 100 °C for three hours using a 1:4 ratio for sample:ultrapure water. The extracted materials were dried on anhydrous sodium sulfate (Sigma-Aldrich, St. Louis, USA), filtered through a 0.22 μm cellulose membrane, and stored in borosilicate glass vials at −20 °C until further analysis.[10]

Characterization of the essential oils

The identification of the copaiba (*Copaifera langsdorffii* Desf.), sacaca (*Croton cajucara* Benth.), and negramina (*Siparuna guianensis* Aublet.) essential oil compounds followed gas chromatography-mass spectrometry (GC-MS) and gas chromatography with flame-ionization detection (GC-FID) methods. The GC-MS analysis occurred into HP 6890 gas chromatograph with split/splitless injection port, combined with an HP-5MS cross-linked fused silica capillary column (30 m × 0.25 mm × 0.25 μm) and HP-5975 mass selective detector (Hewlett-Packard Company, Wilmington, USA). The carrier gas applied was helium. The injection of essential oils corresponded to a volume of 1 μL and a 1:25 split ratio. The chromatographic parameters were: oven initial temperature, 60 °C; ramp rate, 5 °C min⁻¹; oven final temperature, 250 °C; injector, 220 °C; detector, 250 °C. The electron ionization system was set at 70 eV. Data acquisition and integration were carried out through the MSD ChemStation software. The essential oils' components identification applied the comparison of their fragmentation pattern with the National Institute of Standards and Technology (NIST-05) mass spectral library data, the Kovats index, retention index from co-injection of *n*-alkane standard solutions (C_8-C_{20}) (Sigma-Aldrich,

St. Louis, USA), under the same chromatographic conditions.[10] The analyte concentrations were calculated according to their peak areas in the chromatogram.

The GC-FID analysis employed a PR2100 GC-FID instrument with split/splitless injection port (Alpha MOS, Toulouse, France), combined with a fused silica capillary column (30 m × 0.25 mm × 0.25 μm) coated with cross-linked 5% phenyl polysilphenylene-siloxane (SGE Analytical Science Pty Ltd, Victoria, Australia). The chromatographic parameters correspond to those described before to GC-MS. Data acquisition and integration were carried out using Winilab software. β-Caryophyllene, α-humulene, and isoshyobunone were selected as the standard for the quantification of the main components present in the essential oils.[10]

Ligand file selection and preparation

In the search for a relevant ligand-protein interaction, the molecular docking evaluated the main components of the assayed essential oils, considering compounds with concentrations higher than 2%. A total of 31 main sesquiterpenes were identified and then applied against the human pathogenic protein of the SARS-CoV-2 virus, such as SARS-CoV-2 Main Protease, Nsp15/NendoU, RdRp, Spike S, and also the protein hACE2, were considered for the docking *in silico* analysis. The compound's chemical structures were downloaded from NIH-National Library of Medicine (PubChem)[17] in SDF format of the 3-D conformation of all sesquiterpene type-compounds and then converted to a protein data bank (PDB) file by applying OpenBabel[18] software. Afterward, AutoDock Tools 4.2[19] was used to detect the compound roots and structural torsion. Finally, files were saved separately in a PDBQT format file (protein data bank, partial charge "Q" and atom type "T") for further analysis.

Protein preparation

Since the assayed essential oil compounds interacted with SARS-CoV-2 through its target proteins and also hACE2 protein, Swiss-model server[20-22] (a fully automated protein structure homology-modeling server) was then used to find the most suitable templates for the selected target proteins. For this purpose, this server performed a basic local alignment search (BLAST) in order to find regions of similarity between biological sequences, and the best matches. Therefore, a structure comparison becomes possible by using QMEAN analysis. The minimal acceptable resolution for the proteins files was considered as 2.0 Å. Protein structures were downloaded from RCSB-Protein Data Bank[23] after template homology studies. Host proteins were split into five main groups aiming to analyze the molecule's interactions separated by group (Table 1).

Posteriorly, AutoDock Tools (The Scripps Research Institute) properly checked all chemical particularities of each molecule involved in the molecular interaction.[19] The target macromolecules were dehydrated and hydrogens were added afterward only on the polar atoms. Also, Kollman charges were added to the target macromolecules

Table 1. Protein Data Bank (PDB) files separated in five groups by homologues of each studied crystal structure

hACE-2	SARS-CoV-2 Main Protease	SARS-CoV-2 Nsp15/NendoU	SARS-CoV-2 RdRp	SARS-CoV-2 Spike S
–	5R7Z	–	–	–
–	5R80	–	–	–
6M17	5R81	6VWW	–	–
1R42	5R82	6V02	6M71	6M0J
–	5R83	–	–	–
–	5R84	–	–	–
–	6LU7	–	–	–

hACE2 group: 6M17 is a complex composed by the interactions of the angiotensin-converting enzyme 2 (chains B and D), SARS-CoV-2 receptor binding domain (chains E and F) and sodium-dependent neutral amino acid transporter B(0)AT1 (chains A and C).1R42 is the native human angiotensin-converting enzyme-related carboxypeptidase - hACE2 (chain A). SARS-CoV-2 M-pro group: 5R7Z is the 3C-like proteinase, a crystal structure of the SARS-CoV-2 main protease in complex with Z1220452176; 5R80 is the 3C-like proteinase, a crystal structure of the SARS-CoV-2 main protease in complex with Z18197050; 5R81 is the 3C-like proteinase, a crystal structure of the SARS-CoV-2 main protease in complex with Z1367324110; 5R82 is the 3C-like proteinase, a crystal structure of the SARS-CoV-2 main protease in complex with Z219104216; 5R83 is the 3C-like proteinase, a crystal structure of the SARS-CoV-2 main protease in complex with Z44592329; 5R84 is the 3C-like proteinase, a crystal structure of the SARS-CoV-2 main protease in complex with Z31792168; 6LU7 is a crystal structure of the SARS-CoV-2 main protease in complex with an inhibitor N3; 6M03 is a crystal structure of the SARS-CoV-2 main protease in apo form; 6Y84 the SARS-CoV-2 main protease with unliganded active site (2019-nCoV, coronavirus disease 2019, COVID-19). SARS-CoV-2 Nsp15/NendoU group: 6VWW is the crystal structure of NSP-15 endoribonuclease from SARS-CoV-2; 6W01 is a 1.9 Å crystal structure of NSP15 endoribonuclease from SARS-CoV-2 in complex with citrate; 6W02 is a crystal structure of ADP ribose phosphatase of NSP3 from SARS CoV-2 in complex with ADP ribose. SARS-CoV-2 RdRp group: 6M71 is a SARS-CoV-2 RNA-dependent RNA polymerase in complex with cofactors. Spike S group: 6M0J is a crystal structure of the SARS-CoV-2 spike receptor-binding domain bound with hACE2.

and Gasteiger charges were computed, as a common preparation required for further docking on these software.

Molecular docking simulation

A blind docking was initially performed by AutoDock Vina[24] to locate alternate binding sites enclosing the whole macromolecules with a very extended grid (60 Å × 60 Å × 60 Å). So, procedures were achieved for each macromolecule to search the whole interaction sites possibilities by applying exhaustiveness values of 8, 16, 24, 32, 64, 128, and 500. The analysis of an output file composed of 496 individual interaction files, regarding the 31 herbal chemical compounds and 15 host proteins, which were considered among the 20 best VINA score bindings. The best binding energy modes were chosen to rerun separately in their specific binding sites to get precisely the best scores of specific regions to its possible binding poses. In this way, a detailed study was conducted with a smaller grid (44 Å × 32 Å × 48 Å) centered on the groove, with exhaustiveness values of 64 and 3 repetitions for each selected molecule, printing up to 20 modes and results within −5.0 kcal mol^{-1} from the lowest energy pose. Hence, the main molecules with the lowest energy binding level of each group were selected for visual presentation. Also, the energy range was set to 4 for all VINA's files. Due to the huge amount of data involved in this processing thread, the dockME LITE Alpha[25] software was applied. This open source software is just an automated computational tool that makes an interface with Autodock VINA by activating it through terminal command lines automatically, screening every macromolecule contained in the folder against every ligand prepared in another folder.[25]

In addition, PyMol software[26] was also used for the best binding sites visualization. Meanwhile, the APBS (Adaptive Poisson-Boltzmann Solver) model was then assessed for electrostatics and solvation complementary analysis due to its accuracy to determine the electrostatic energy under polar solvent conditions. For the automatic generation of 2D ligand-protein interaction, LigPlot+ software[27] was applied to depict hydrophobic bonds, hydrogen bonds, and their bond lengths in each docking pose in the form of graphical representation.

Results and Discussion

Essential oils composition

GC-MS and GC-FID analysis showed a total of 31 main sesquiterpenes from *Copaifera langsdorffii* Desf.,

Croton cajucara Benth., and *Siparuna guianensis* Aublet. which contents higher than 2% corresponded to over 78% of the found sesquiterpenes (Table 2).

The main sesquiterpenes from *C. langsdorffii* were β-bisabolene (23.6%), β-caryophyllene (21.7%), and α-bergamotene (20.5%) being in accordance with previous reports from *Copaifera* specimens.[10,28,29] Linalool (42.3%) and (*E*)-nerolidol (13.6%) were identified for *C. cajucara*. Otherwise, the previous analysis showed linalool (13.5%), γ-muurolene (18.4%), and (*Z*)-sesquilavandulol (12.6%)[30] as the main essential oil components of *C. cajucara* leaves. Additionally, 7-hydroxy calamenene (37.5 to 28.4%), α-pinene (24.7 to 0.1%), linalool (13.2 to 6.3%), and β-caryophyllene (5.7 to 2.6%) were registered on different essential oil samples from *C. cajucara* leaves, as the majority components.[31]

Concerning to *S. guianensis* specimen more elevated sesquiterpene concentration was shyobunone and its derivatives iso-shyobunone (23.9%) and epi-shyobunone (18.9%). Moreover, Valentini *et al.*[16] obtained oils with the predominance of siparunone oxygenated sesquiterpenes, while Aguiar *et al.*[15] registered higher concentrations of β-myrcene (79.71%) and 2-undecanone (14.58%). Indeed, the differences in the composition and contents of natural essential oils is common and oscillates due to the stage in the vegetative cycle, plant organ, age of the plant, extraction process and also environmental conditions, such as the climate of the region, season, and also by the soil composition.[5,10]

Molecular docking simulation

Molecular docking methods predicted the ligand interactions with macromolecules identified for SARS-CoV-2, which may represent potential targets for chemotherapeutic intervention. The blind docking method involves a search throughout the entire surface of the macromolecule for binding sites. Herein, the 31 sesquiterpenes compounds (Table 2) were screened to the main proteins involved in the SARS-CoV-2 resistance (hACE2) and infection (SARS-CoV-2 M-Pro, SARS-CoV-2 Nsp15/NendoU, SARS-CoV-2 RdRP, and Spike S).

Facing COVID-19 disease, as utmost need, previous reports have shown molecular docking approaches to search natural compounds against SARS-CoV-2 infections.[1,27] From this perspective, concerning *Copaifera langsdorffii* Desf., *Croton cajucara* Benth., and *Siparuna guianensis* Aublet., the best ligand-protein binding energy to perform molecular docking were obtained according to Table 3.

According to Table 3, the finds showed that the assessed sesquiterpenes possessed negative values of the binding

Table 2. Chromatography data of the essential oils from *Copaifera langsdorffii* Desf., *Croton cajucara* Benth., and *Siparuna guianensis* Aublet
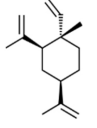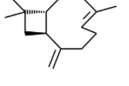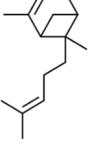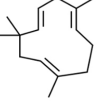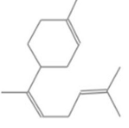
Plant source	Sesquiterpene	PubChem ID	Chemical structure	Kovats retention index	Concentration / %
Copaifera langsdorffii Desf.	β-elemene	10583		1392	2.0
	β-caryophyllene	62127		1421	21.7
	α-bergamotene	86608		1437	20.5
	α-humulene	3015263		1453	2.9
	β-farnesene	10407		1457	1.7
	germacrene D	5317570		1481	1.7
	β-selinene	442393		1486	6.1
	α-selinene	10123		1494	2.3
	β-bisabolene	10104370		1510	23.6
	caryophyllene oxide	1742210		1583	4.1
Croton cajucara Benth.	linalool	6549		1100	42.3
	β-bourbonene	62566		1386	2.1
	β-caryophyllene	62127		1421	6.5
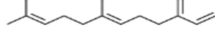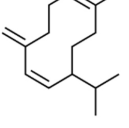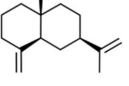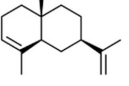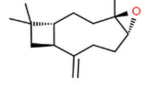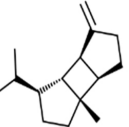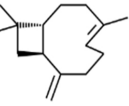
Table 2. Chromatography data of the essential oils from *Copaifera langsdorffii* Desf., *Croton cajucara* Benth., and *Siparuna guianensis* Aublet (cont.)
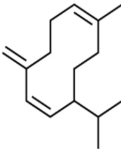
Plant source	Sesquiterpene	PubChem ID	Chemical structure	Kovats retention index	Concentration / %
	germacrene D	5317570		1481	4.4
	bicyclogermacrene	13894537		1491	2.5
Croton cajucara Benth.	germacrene B	5281519		1554	2.4
	(*E*)-nerolidol	5284507		1561	13.6
	spathulenol	92231		1570	2.2
	caryophyllene oxide	1742210		1582	2.0
	shyobunone	5321293		1492	2.7
	α-muurolene	12306047		1503	6.1
Siparuna guianensis Aublet.	guaiene	6949		1508	4.1
	epishyobunone	591309		1525	18.9
	δ-cadinene	441005		1534	2.2
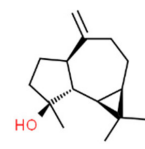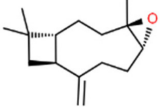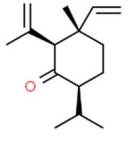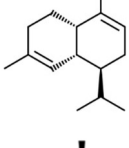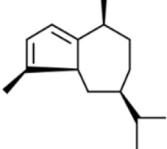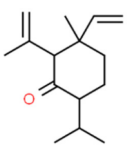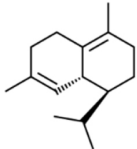
Table 2. Chromatography data of the essential oils from *Copaifera langsdorffii* Desf., *Croton cajucara* Benth., and *Siparuna guianensis* Aublet (cont.)
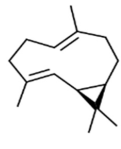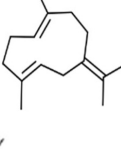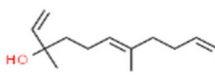
Plant source	Sesquiterpene	PubChem ID	Chemical structure	Kovats retention index	Concentration / %
Siparuna guianensis Aublet.	elemol	92138		1566	3.6
	spathulenol	92231		1572	3.7
	iso-shyobunone	5318673		1611	23.9
	γ-eudesmol	6432005		1649	4.8
	t-muurolol	3084331		1654	5.1
	epi-α-bisabolol	1201551		1700	2.2
	farnesyl acetate	638500		1895	2.2
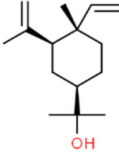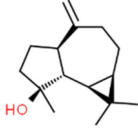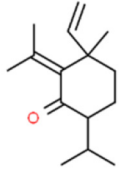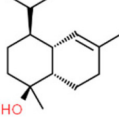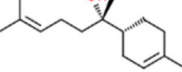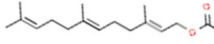
affinity playing an important role in the inhibition of the macromolecules. Indeed, previous studies predict that compounds with a binding affinity lower to −6.5 kcal mol⁻¹ or less acting on active sites have shown effective proteins inhibition under significant stability of the ligand-protein complex.[32,33]

It was also evidenced that the assessed plants have shown a good quantity of sesquiterpenes with considerably acceptable negative binding affinities with the selected targets of SARS-CoV-2 proteins. Moreover, sesquiterpenes of *S. guianensis* showed significant single or multiple interactions with some SARS-CoV-2 proteins. Otherwise, weak or no relevant interaction with any SARS-CoV-2 proteins was observed for α-bergamotene and germacrene D (*C. langsdorffii*), as well as linalool and germacrene D (*C. cajucara*). Meanwhile, higher binding affinities were obtained between SARS-CoV-2 M-Pro with β-selinene (−7.2 kcal mol⁻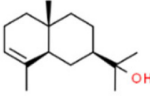¹) or γ-eudesmol (−7.5 kcal mol⁻¹), from *C. langsdorffii* and *S. guianensis*, respectively. SARS-CoV-2 M-Pro corresponds to the primary enzyme responsible for processing the polyproteins translated from the viral RNA.[4,29]

Sesquiterpenes from *C. cajucara* presented a higher binding affinity (−7.1 kcal mol⁻¹) to spathulenol-hACE2, which is an important receptor for viral entrance in human cells.[2,4,5] For SARS-CoV-2 RdRP, sesquiterpenes from *C. langsdorffii* and *S. guianensis* did not present significant binding energy. On the other hand, bicyclogermacrene (*C. cajucara*) were able to interact with this protein, which is a target polymerase responsible for the viral genome replication within the host cells.[4] At this point, it is important that these inhibition effects on the SARS-CoV-2 main target proteins are encouraging to consider the Brazilian essential oils (*C. langsdorffii*, *C. cajucara*, and *S. guianensis*) or its isolated compounds to further studies aiming at to formulate adjuvants against SARS-CoV-2.

The top-ranked interaction between sesquiterpenes from essential oils with amino acids of SARS-CoV-2 inhibitors were described at the Table 4, in which: (*i*) PDB1R42 is the native human angiotensin-converting enzyme-related

Table 3. Binding affinity obtained by molecular docking for the interaction among sesquiterpenes identified from the Brazilian essential oils and severe acute respiratory syndrome coronavirus 2 (SARS-CoV-2) molecular targets (hACE2, SARS-CoV-2 M-Pro, SARS-CoV-2 Nsp15/NendoU, SARS-CoV-2 RdRp, and Spike S)

| Plant source | Sesquiterpene | Binding affinity / (kcal mol^{-1}) | | | | | | | | | | | | | | | |
| | | hACE2 | | SARS-CoV-2 M-Pro | | | | | | | | | SARS-CoV-2 Nsp15/NendoU | | | SARS-CoV-2 RdRp | Spike S |
		6M17	1R42	5R7Z	5R80	5R81	5R82	5R83	5R84	6LU7	6M03	6Y84	6VWW	6W01	6W02	6M71	6M0J
C. langsdorffii Desf.	β-elemene	−6.1	−6.0	−5.2	−5.5	−5.2	−5.4	−5.2	−5.4	−5.5	−5.8	−6.7	−5.8	−5.5	−5.3	−5.8	−5.7
	β-caryophyllene	−6.6	−6.5	−5.7	−5.6	−5.8	−5.6	−5.6	−5.6	−5.9	−6.3	−6.6	−6.3	−5.8	−5.5	−6.3	−6.2
	α-bergamotene	−6.3	−6.0	−5.0	−5.7	−5.5	−5.7	−4.8	−5.9	−5.6	−5.7	−6.3	−6.0	−5.8	−5.0	−5.8	−6.0
	α-humulene	−6.3	−6.4	−5.7	−5.8	−6.0	−5.4	−5.3	−5.6	−6.1	−6.2	−6.6	−6.1	−6.2	−5.3	−6.4	−6.1
	β-farnesene	−6.0	−6.1	−5.1	−4.7	−4.1	−5.0	−4.8	−4.4	−4.8	−4.7	−6.6	−5.1	−5.6	−5.3	−5.2	−6.3
	germacrene D	−6.1	−5.9	−5.5	−5.4	−5.5	−5.5	−5.4	−5.4	−5.6	−6.0	−6.2	−6.0	−6.1	−5.0	−5.6	−5.6
	β-selinene	−6.8	−7.0	−6.1	−6.1	−6.0	−6.0	−5.9	−5.9	−6.2	−6.3	−7.2	−6.3	−6.1	−5.6	−6.0	−6.7
	α-selinene	−6.7	−6.7	−5.7	−6.0	−6.0	−6.0	−6.0	−4.7	−6.2	−6.4	−6.5	−6.3	−6.9	−5.5	−6.2	−6.4
	β-bisabolene	−5.2	−5.9	−4.7	−5.4	−4.8	−4.6	−4.5	−5.9	−5.4	−5.7	−6.6	−5.7	−6.1	−4.4	−4.9	−6.8
	caryophyllene oxide	−6.7	−6.8	−6.0	−5.8	−6.2	−6.1	−6.1	−5.3	−6.0	−6.3	−6.8	−6.2	−6.9	−5.5	−6.0	−6.6
C. cajucara Benth.	linalool	−5.1	−4.9	−4.4	−4.6	−4.1	−4.6	−4.5	−4.5	−4.1	−4.6	−5.8	−5.5	−5.0	−4.4	−4.6	−5.2
	β-bourbonene	−6.7	−6.7	−6.2	−5.8	−6.0	−6.3	−6.0	−5.9	−6.1	−6.4	−6.8	−6.1	−6.8	−5.7	−6.2	−6.7
	β-caryophyllene	−6.6	−6.5	−5.7	−5.6	−5.8	−5.6	−5.6	−5.6	−5.9	−6.3	−6.6	−6.3	−5.8	−5.5	−6.3	−6.2
	germacrene D	−6.1	−5.9	−5.5	−5.4	−5.5	−5.5	−5.4	−5.4	−5.6	−6.0	−6.2	−6.0	−6.1	−5.0	−5.6	−5.6
	bicyclogermacrene	−7.0	−6.4	−5.5	−6.0	−5.8	−5.6	−5.7	−6.0	−6.0	−6.6	−6.7	−6.3	−6.1	−5.7	−6.7	−6.7
	germacrene B	−6.4	−6.7	−5.6	−5.6	−5.6	−5.5	−5.6	−5.5	−5.9	−6.3	−6.6	−6.3	−6.2	−5.5	−6.1	−6.3
	(*E*)-nerolidol	−5.7	−5.4	−4.9	−5.2	−5.1	−5.3	−5.1	−5.6	−5.0	−6.0	−7.0	−5.3	−5.3	−5.1	−5.3	−5.6
	spathulenol	−7.0	−7.1	−6.0	−5.8	−5.6	−5.8	−6.4	−5.8	−6.3	−6.4	−6.9	−6.3	−6.3	−6.2	−6.3	−6.6
	caryophyllene oxide	−6.7	−6.8	−6.0	−5.8	−6.2	−6.1	6.1	−5.3	−6.0	−6.3	−6.8	−6.2	−6.9	−5.5	−6.0	−6.6
S. guianensis Aublet.	shyobunone	−5.8	−6.1	−5.6	−5.4	−5.2	−5.2	−5.6	4.5	−5.5	−5.9	−6.8	−5.8	−6.5	−5.1	−5.8	−5.9
	α-muurolene	−6.7	−6.8	−6.1	−6.4	−6.2	−6.2	−5.8	−6.3	−6.1	−6.6	−6.3	−6.3	−7.1	−5.5	−6.3	−6.6
	guaiene	−6.7	−6.4	−6.2	−6.0	−6.1	−6.1	−6.1	−6.1	−6.2	−6.4	−6.7	−6.2	−6.5	−5.8	−6.1	−6.4
	epishyobunone	−6.1	−5.9	−5.4	−5.3	−4.5	−5.1	−5.0	−5.1	−5.6	−5.9	−6.7	−5.7	−6.3	−5.1	−5.7	−5.7
	δ-cadinene	−6.4	−6.6	−5.7	−5.7	−6.0	−5.6	−5.6	−6.0	−6.0	−6.2	−6.8	−6.7	−6.8	−5.7	−6.2	−6.8
	elemol	−6.0	−6.2	−5.4	−5.6	−5.8	−5.6	−5.6	−5.6	−6.0	−6.2	−6.9	−5.9	−6.4	−5.4	−5.9	−5.8
	spathulenol	−7.0	−7.1	−6.0	−5.8	−5.6	−5.8	−6.4	−5.8	−6.3	−6.4	−6.9	−6.3	−6.3	−6.2	−6.3	−6.6
	iso-shyobunone	−6.4	−6.2	−5.5	−5.8	−5.9	−5.8	−5.8	−6.0	−5.8	−5.9	−6.6	−6.3	−5.9	−5.6	−6.1	−5.8
	γ-eudesmol	−7.0	−7.2	−5.9	−5.4	−6.1	−6.1	−5.8	−6.1	−6.4	−6.8	−7.5	−6.6	−7.3	−5.7	−6.3	−6.5
	t-muurolol	−6.6	−6.5	−6.2	−6.3	−6.1	−6.2	−6.1	−6.1	−5.9	−6.5	−7.4	−6.7	−6.4	−5.8	−6.0	−7.1
	epi-α-bisabolol	−6.5	−6.5	−5.4	−5.3	−5.5	−5.7	−5.3	−5.8	−5.3	−5.4	−7.3	−6.4	−6.5	−5.3	−6.2	−6.8
	farnesyl acetate	−5.9	−5.9	−5.6	−5.3	−5.5	−5.1	−5.3	−5.2	−5.2	−6.0	−6.7	−6.3	−4.6	−4.9	−5.0	−6.3

hACE2 group: 6M17 is a complex composed by the interactions of the angiotensin-converting enzyme 2 (chains B and D), SARS-CoV-2 receptor binding domain (chains E and F) and sodium-dependent neutral amino acid transporter B(0)AT1 (chains A and C).1R42 is the native human angiotensin-converting enzyme-related carboxypeptidase - hACE2 (chain A). SARS-CoV-2 M-pro group: 5R7Z is the 3C-like proteinase, a crystal structure of the SARS-CoV-2 main protease in complex with Z1220452176; 5R80 is the 3C-like proteinase, a crystal structure of the SARS-CoV-2 main protease in complex with Z18197050; 5R81 is the 3C-like proteinase, a crystal structure of the SARS-CoV-2 main protease in complex with Z1367324110; 5R82 is the 3C-like proteinase, a crystal structure of the SARS-CoV-2 main protease in complex with Z219104216; 5R83 is the 3C-like proteinase, a crystal structure of the SARS-CoV-2 main protease in complex with Z44592329; 5R84 is the 3C-like proteinase, a crystal structure of the SARS-CoV-2 main protease in complex with Z31792168; 6LU7 is a crystal structure of the SARS-CoV-2 main protease in complex with an inhibitor N3; 6M03 is a crystal structure of the SARS-CoV-2 main protease in apo form; 6Y84 the SARS-CoV-2 main protease with unliganded active site (2019-nCoV, coronavirus disease 2019, COVID-19). SARS-CoV-2 Nsp15/NendoU group: 6VWW is the crystal structure of NSP-15 endoribonuclease from SARS-CoV-2; 6W01 is a 1.9 Å crystal structure of NSP15 endoribonuclease from SARS-CoV-2 in complex with citrate; 6W02 is a crystal structure of ADP ribose phosphatase of NSP3 from SARS CoV 2 in complex with ADP ribose. SARS-CoV-2 RdRp group: 6M71 is a SARS-CoV-2 RNA-dependent RNA polymerase in complex with cofactors. Spike S group: 6M0J is a crystal structure of the SARS-CoV-2 spike receptor-binding domain bound with hACE2.

carboxypeptidase-hACE2; (*ii*) chain A is related to the SARS-Cov-2 NSP 12, while chain C is related to the SARS-CoV-2 NSP 8; (*iii*) chain A are related to ACE2 receptors, while chain E corresponds to the spike receptor-binding domain, and B and D amino acid chains correspond to the SARS-CoV-2 NSP 7; (*iv*) PDB6Y84 is the SARS-CoV-2 main protease with unliganded active site (2019-nCoV, coronavirus disease 2019, COVID-19), related to the

replicase polyprotein 1ab; (*v*) PDB6W01 is a 1.9 Å crystal structure of NSP15 endoribonuclease from SARS-CoV-2 in complex with a citrate and its crystal structures are related to the uridylate-specific endoribonuclease; (*vi*) PDB6M71 is a SARS-CoV-2 RNA-dependent RNA polymerase in complex with cofactors; (*vii*) PDB6M0J is a crystal structure of SARS-CoV-2 spike receptor-binding domain bound with ACE2.

As result, the higher binding affinities were found to γ-eudesmol and t-muurolol (*S. guianensis*) with

Table 4. Top ranked sesquiterpenes from Brazilian essential oils screened against proteins involved in the SARS-CoV-2 infection emphasizing the receptor-binding residues

Plant source	Protein group	Macromolecule PDB	Terpenes with the lowest binding level	Energy level / (kcal mol^{-1})	Residues interacting with phytochemical through H-bonding and other interactions related to chains A and B
C. langsdorffii Desf.	hACE2	1R42	β-selinene	−7.0	Asn159 (A) Trp163 (A) Pro135 (A) Asn134 (A) Glu160 (A)
	SARS-CoV-2 M-Pro	6Y84	β-selinene	−7.2	Lis5 (A) Phe291 (A) Glu288 (A) Trp207 (A) Leu282 (A) Phe3 (A) Arg4 (A)
	SARS-CoV-2 Nsp15/NendoU	6W01	α-selinene	−6.9	Asp297 (B) Val295 (B) Thr275 (B) Ser274 (B) Ser198 (B) Lys90 (B) Asn200 (B) Tyr279 (B) Leu252 (B) Arg199 (B) Ile296 (B) Lys277 (B)
			caryophyllene oxide		Lys71 (B) (2.96 Å) Asp273 (B) Asp297 (B) Arg199 (B) Leu252 (B) Lys277 (B) Tyr279 (B) Asn200 (B)
	SARS-CoV RdRp	6M71	α-humulene	−6.4	Arg116 (A) Val71 (A) Asp218 (A) Tyr217 (A) Lys50 (A) Arg33 (A) Phe35 (A) Ala34 (A) Thr123 (A) Asp208 (A)
	Spike S	6M0J	β-bisabolene	−6.8	Ala413 (A) MET366 (A) Thr434 (A) Glu430 (A) Pro415 (A) Glu435 (A) Ile291 (A) Asn290 (A) Phe438 (A)
C. cajucara Benth.	hACE2	1R42	spathulenol	−7.1	Pro612 (A) Tyr158 (A) Pro490 (A) Leu162 (A) Val491 (A) Tyr613 (A)
	SARS-CoV-2 M-Pro	6Y84	(*E*)-nerolidol	−7.0	Glu290 (2.78 Å) (A) Gln127 (2.76 Å) (A) Arg4 (A) Phe3 (A) Phe291 (A) Trp207 (A) Glu288 (A) Lys5 (2.94 Å) (A) Lys137 (A)
	SARS-CoV-2 Nsp15/NendoU	6W01	caryophyllene oxide	−6.9	Pro206 (B) Phe204 (B) Ala256 (B) Lys260 (B) Leu215 (B)
	SARS-CoV RdRp	6M71	bicyclogermacrene	−6.7	Tyr217 (A) Arg116 (A) Val71 (A) Thr123 (A) Arg33 (A) Phe35 (A) Asp208 (A) Asn209 (A)
	Spike S	6M0J	β-bourbonene	−6.7	Ser47 (A) Ser44 (A) Asp350 (A) Phe40 (A) Thr347 (A) Ala348 (A) Trp349 (A)
			bicyclogermacrene		Phe40 (A) Phe390 (A) Trp69 (A) Asn394 (A) Leu391 (A) Arg393 (A)
S. guianensis Aublet.	hACE2	1R42	γ-eudesmol	−7.2	Ala396 (3.10Å) (A) Glu564 (2.88Å) (A) Trp566 (A) Glu208 (A) Pro565 (A) Asp206 (A) Val209 (A) Gln98 (A) Ala99 (A) Lys562 (A) Leu95 (A)
	SARS-CoV-2 M-Pro	6Y84	γ-eudesmol	−7.5	Glu290 (2.70Å) (A) Lys5 (2.91Å) (A) Gln127 (2.97Å) (A) Lys137 (A) Glu288 (A)
	SARS-CoV-2 Nsp15/NendoU	6W01	γ-eudesmol	−7.3	Tyr279 (2.83Å) (B) Lys277 (B) Asp297 (B) Thr275 (B) Ser274 (B) Lys71 (B) Asp273 (B) Lys90 (B) Ser198 (B) Asp268 (B)
	SARS-CoV RdRp	6M71	γ-eudesmol	−6.3	Ser397 (2.83Å and 2.96Å) (A) Cys395 (2.89Å) (A) Leu389 (A) Thr394 (A) Thr324 (A) Phe396 (A) Tyr149 (B) Leu122 (B)
			spathulenol		Ser709 (3.21Å) (A) His133 (2.98Å) (A) Tyr129 (3.01Å) (A) Ser784 (A) Asn781 (A) Lys47 (A) Asp135 (A) Lys780 (A)
			α-muurolene		Tyr546 (A) Leu544 (A) Thr409 (A) Val410 (A) Lys411 (A) Asp845 (A) Ile847 (A)
	SPIKE S	6M0J	t-muurolol	−7.1	Arg393 (2.78Å) (A) Asp350 (A) Phe40 (A) GLY352 (A) Phe390 (A) Trp69 (A) Asn394 (A)

PDB: protein database; hACE2 group: 6M17 is a complex composed by the interactions of the angiotensin-converting enzyme 2 (chains B and D), SARS-CoV-2 receptor binding domain (chains E and F) and sodium-dependent neutral amino acid transporter B(0)AT1 (chains A and C).1R42 is the native human angiotensin-converting enzyme-related carboxypeptidase - hACE2 (chain A). SARS-CoV-2 M-pro group: 5R7Z is the 3C-like proteinase, a crystal structure of the SARS-CoV-2 main protease in complex with Z1220452176; 5R80 is the 3C-like proteinase, a crystal structure of the SARS-CoV-2 main protease in complex with Z18197050; 5R81 is the 3C-like proteinase, a crystal structure of the SARS-CoV-2 main protease in complex with Z1367324110; 5R82 is the 3C-like proteinase, a crystal structure of the SARS-CoV-2 main protease in complex with Z219104216; 5R83 is the 3C-like proteinase, a crystal structure of the SARS-CoV-2 main protease in complex with Z44592329; 5R84 is the 3C-like proteinase, a crystal structure of the SARS-CoV-2 main protease in complex with Z31792168; 6LU7 is a crystal structure of the SARS-CoV-2 main protease in complex with an inhibitor N3; 6M03 is a crystal structure of the SARS-CoV-2 main protease in apo form; 6Y84 the SARS-CoV-2 main protease with unliganded active site (2019-nCoV, coronavirus disease 2019, COVID-19). SARS-CoV-2 Nsp15/NendoU group: 6VWW is the crystal structure of NSP-15 endoribonuclease from SARS-CoV-2; 6W01 is a 1.9 Å crystal structure of NSP15 endoribonuclease from SARS-CoV-2 in complex with citrate; 6W02 is a crystal structure of ADP ribose phosphatase of NSP3 from SARS CoV-2 in complex with ADP ribose. SARS-CoV-2 RdRp group: 6M71 is a SARS-CoV-2 RNA-dependent RNA polymerase in complex with cofactors. Spike S group: 6M0J is a crystal structure of the SARS-CoV-2 spike receptor-binding domain bound with hACE2.

hACE2 (PDB 1R42), SARS-CoV-2 M-Pro (PDB 6Y84), SARS-CoV-2 Nsp15/NendoU (PDB 6W01), and Spike S (PBD6M0J). Comparatively, *C. cajucara* and *C. langsdorffii* essential oils held the best inhibitory activity against hACE2 (PDB 1R42). On the other hand, bicyclogermacrene (*C. cajucara*) registered the best inhibition results for SARS-CoV RdRp (PDB 6M71).

Once SARS-CoV-2 protein is placed on the hACE2 receptor (PDB 6M17), the binding energy of the interaction with the sesquiterpenes may decrease (Table 3). This effect suggests that sesquiterpenes interact in the native human angiotensin-converting enzyme site, decreasing the interactions with the SARS-CoV-2 receptor. In this perspective, *S. guianensis* essential oil holds a higher binding affinity to SARS-CoV-2 M-Pro. This result indicates that γ-eudesmol acts in the main protease of coronaviruses responsible for mediating viral replication and transcription.[29] According to Table 4, it was also possible to determine that sesquiterpenes mainly interacted spontaneously with the amino acid residues through hydrophobic interactions and also promotes few hydrogen bonding above 3.21 Å.

It is noteworthy that some compounds may present an inhibitory effect on several proteins simultaneously, and the analyzed sesquiterpenes also displayed equal binding energy for the same protein. These data suggest that the evaluated components of the Brazilian essential oils can be used *in natura* in further *in vitro* and *in vivo* studies as options to be considered to treat or prevent synergistically the coronavirus, as well as in form of isolated sesquiterpenes since some of them acted directly in one or multiple SARS-CoV-2 proteins. It is also possible to confirm that all the studied herbal oils have presented meaningful binding energy levels in its solvation process with the target proteins that they were docked, with an energy level lower than −5.4 kcal mol⁻¹ (Figure 1a), also noticed when this evaluation is conducted isolated by group (Figure 1b), having the highest meaningful binding energy level result of −5.3 kcal mol⁻¹, therefore, corroborating with Figure 1.

The presented binding energy levels are also observed when data were evaluated in a Gaussian (or Normal distribution):

$$p(x) = \frac{1}{\sigma\sqrt{2\pi}} e^{-\frac{1}{2}\left(\frac{x-\mu}{\sigma}\right)^2} \tag{1}$$

where μ is the expected value of a finite case, calculated as $\mu = E[X] = \sum_{i=1}^{\infty} x_i p(x_i)$; and σ is the standard deviation (Figure 2).

Those results corroborate with Silva *et al.*[1] that performed molecular docking of essential oils compounds against SARS-CoV-2 targets and suggested that these
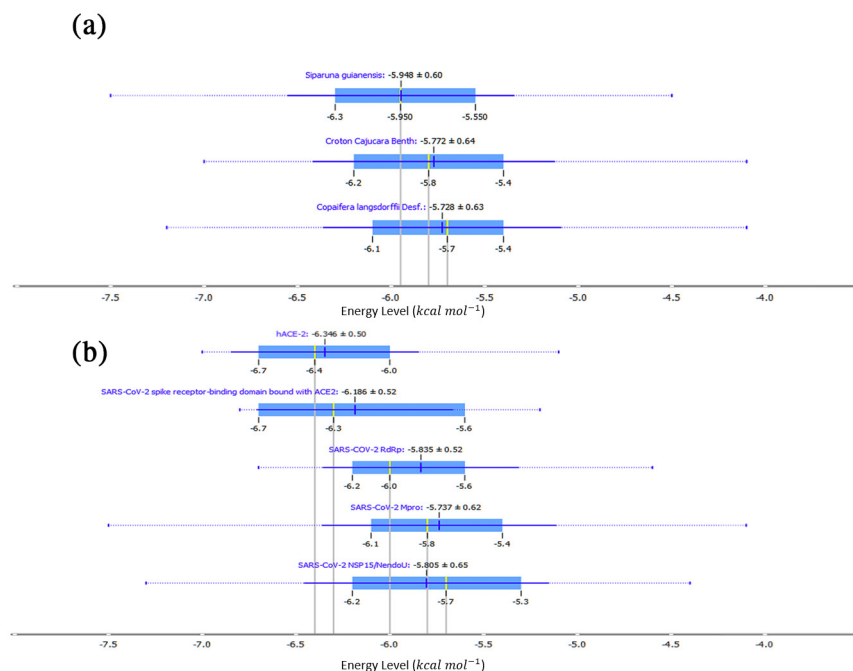

Figure 1. Binding energies of essential oils *versus* the main assayed virus virus targets, where "x̲" is the mean and its standard error and "M" is the median. (a) Binding energy range of each essential oil against all the studied targets (*S. guianensis* x̲ = −5.948 ± 0.60 kcal mol⁻¹ and M = −5.950 kcal mol⁻¹; *C. cajucara* x̲ = −5.772 ± 0.64 kcal mol⁻¹ and M = −5.80 kcal mol⁻¹; *C. langsdorffii* x̲ = −5.728 ± 0.6 kcal mol⁻¹ and M = −5.7 kcal mol⁻¹); (b) Binding energy of all essential oils studied against the main target groups. hACE-2 (x̲ = −6.346 ± 0.50 kcal mol⁻¹ and M = −6.40 kcal mol⁻¹); SARS-CoV-2 Spike S (x̲ = −6.186 ± 0.52 kcal mol⁻¹ and M = −6.30 kcal mol⁻¹); SARS-CoV-2 RdRp (x̲ = −5.835 ± 0.52 kcal mol⁻¹ and M = −6.0 kcal mol⁻¹); SARS-CoV-2 M_pro (x̲ = −5.737 ± 0.62 kcal mol⁻¹ and M = −5.80 kcal mol⁻¹) and SARS-CoV-2 NSP15/NendoU (x̲ = −5.805 ± 0.65 kcal mol⁻¹ and M = −5.70 kcal mol⁻¹).
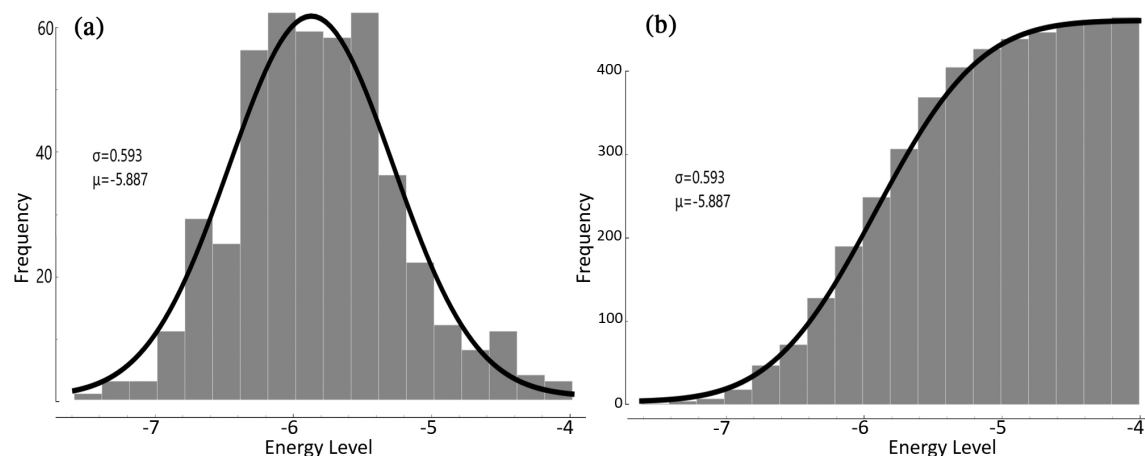
Figure 2. Normal distribution of the binding energy levels of the analyzed compounds. (a) Normal distribution of all binding energy levels ($\mu = -5.887$, $\sigma = 0.593$); (b) cumulative distribution of all the binding energy levels analyzed ($\mu = -5.887$, $\sigma = 0.593$).

substances may act synergistically, amplifying other antiviral agents, and relieving some disease symptoms[1] (Table 4). Indeed, it is also possible to analyze through the normal distribution above described from which more than 90% of the evaluated data presented a binding energy level lower than -5.0 kcal mol^{-1}. This find suggests that the assayed sesquiterpenes applied through an appropriate pharmacological approach may reach the

expected synergic effect against the main proteins of SARS-CoV-2.

Molecular docking analysis

Sesquiterpenes from *C. langsdorffii* showed six main interactions with proteins analyzed by the molecular docking, according to Figure 3.
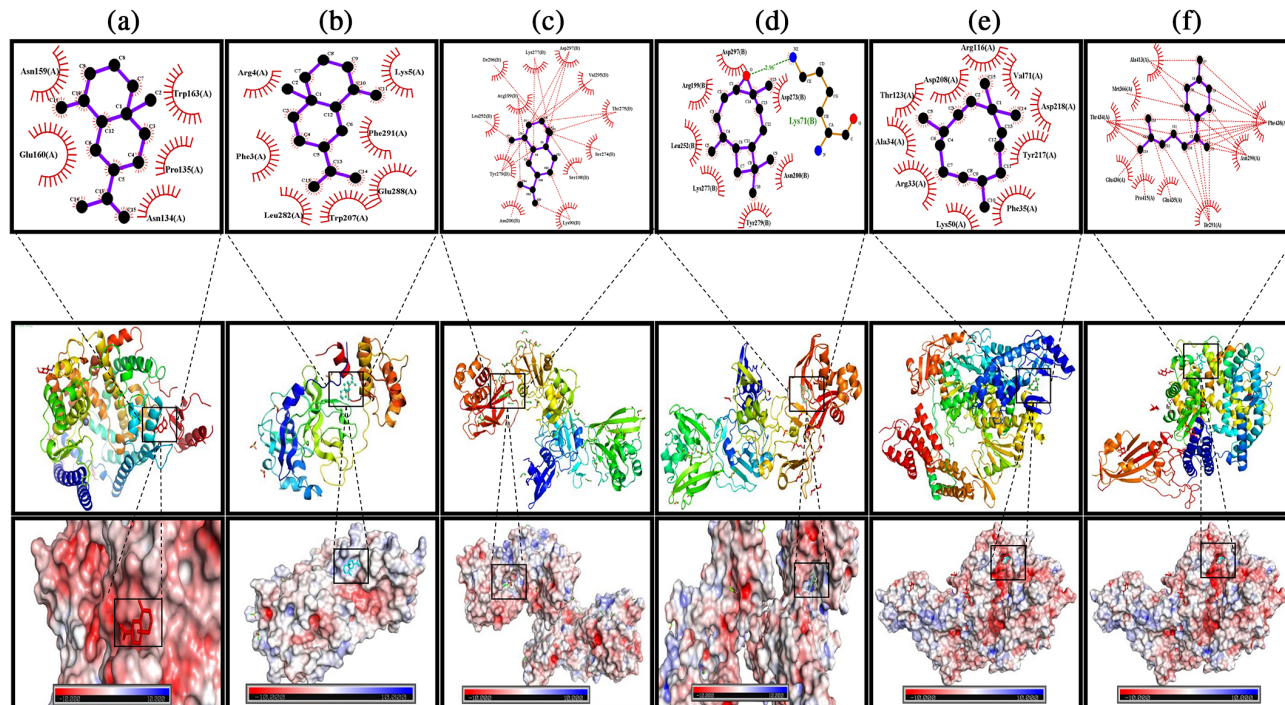

Figure 3. Molecular docking and APBS (adaptive Poisson-Boltzmann solver) solvation of *C. langsdorffii* against the main assayed virus and host domains. (a) Interaction of the ACE 2 with the β-selinene molecule and its APBS solvation; (b) interaction of the SARS-CoV-2 main protease with unliganded active site with the β-selinene molecule and its APBS solvation; (c) interaction of the 1.9 Å crystal structure of NSP15 endoribonuclease from SARS-CoV-2 in the complex with a citrate with the α-selinene molecule and its APBS solvation; (d) interaction of the 1.9 Å crystal structure of NSP15 endoribonuclease from SARS-CoV-2 in the complex with a citrate with the caryophyllene oxide molecule and its APBS solvation; (e) interaction of the SARS-Cov-2 RNA-dependent RNA polymerase in complex with cofactors with the α-humulene and its APBS solvation; (f) interaction of the crystal structure of SARS-CoV-2 spike receptor-binding domain bound with ACE2 with the β-bisabolene and its APBS solvation.

The best affinity energies, binding sites, and electrostatic solvation for *C. langsdorffii* were evidenced for: (*i*) β-selinene interacting with hACE2 and SARS-CoV-2 M-Pro; (*ii*) α-selinene with SARS-CoV-2 Nsp15/NendoU; (*iii*) α-humulene with SARS-CoV RdRp; and (*iv*) β-bisabolene with Spike S. Additionally, among the other ten sesquiterpene ligands, β-selinene held the best binding affinity (−7.0 kcal mol⁻¹) forming the complex β-selinene-ACE2 (PDB: 1R42) (Figure 3a). Meanwhile, β-bisabolene the major compound from copaiba essential oil, showed higher binding energy when complexed with the ACE2 PDB: 6M17 (−5.2 kcal mol⁻¹) and PDB: 1R42 (−5.9 kcal mol⁻¹).

The assayed sesquiterpenes from these Brazilian essential oils showed meaningful docking values indicating that these natural compounds can be directed to the human protein and decrease its binding with the protein virus, and now becoming promising candidates to inhibit both hACE2 isolated (PDB: 1R42) and 2019-nCoV RDB/hACE2-B0AT1 complex (PDB: 6M17). It was possible to predict that there are five main amino acid hydrophobic interactions occurring in the peptidase M2 at domain 3 closest to the disulfide bond of the macromolecule. Moreover, APBS solvation analysis showed strong binding in the very electronegative site on the electrostatic surface of this complex, showing a higher affinity level at these physical conditions.

From nine macromolecules related to SARS-CoV Main Protease, the best energy binding levels were taken from the PDB: 6Y84 with the β-selinene as a ligand, reaching the binding energy level of −7.2 kcal mol⁻¹ on its interaction (Figure 3b and Table 3). So, among ten other compounds from copaiba oil, β-selinene was chosen due to its lowest binding energy level. However, for this protein, it is important to point out that all tested sesquiterpenes showed promising results with a very narrow difference range among its binding values. Concerning the Main Protease group, PDB: 6Y84, β-selinene showed the best binding result, while for PDB: 5R84 it was found as the weakest result. APBS solvation data showed that this molecule binds with an isocontour on electrostatic potential surface. Additionally, β-selinene is bound with seven amino acids making hydrophobic bonds from the PDB: 6Y84 macromolecule: Lis5, Phe291, Glu288, Trp207, Leu282, Phe3, and Arg4. It is also relevant to point out that among the other eight host molecules analyzed, copaiba oil presented the best energy binding levels to 6Y84-macromolecule. Taken all results together, sesquiterpenes from copaiba essential oil are the best inhibitor candidates for further *in vitro* or *in vivo* studies against SARS-CoV Main Protease (M-Pro), being in accordance with other structures of M-Pro from SARS-CoV-2.[34]

Concerning the docking of copaiba essential oil SARS-CoV-2 Nsp15/NendoU protein, the lowest energy binding levels corresponded to α-selinene and caryophyllene oxide ligands with PDB: 6W01 macromolecule (−6.9 kcal mol⁻¹) (Figures 3c and 3d). β-Bisabolene showed a weaker binding affinity with PDB: 6W02 (−4.4 kcal mol⁻¹) and α-selinene was hydrophobically bound with 12 amino acids from the PDB: 6W01: Asp297, Val295, Thr275, Ser274, Ser198, Lys90, Asn200, Tyr279, Leu252, Arg199, Ile296, and Lys277.

Caryophyllene oxide ligand registered interaction with seven amino acids from the crystal structure of NSP15 endoribonuclease from SARS-CoV-2 (PDB ID: 6W01), which are: Asp273, Arg199, Leu252, Lys277, Asn200, Lys71 (H-bound of 2.96 Å), and Tyr279. Both chains (A and B) are related to the uridylate-specific endoribonuclease.[35] In addition, a hydrogen bond at 2.96 Å was verified between the caryophyllene oxide and the Lys71 segment of the SARS-CoV-2 Nsp15/NendoU protein, suggesting strong inhibition. APBS solvation indicated binding at neutral electrostatic sites in both molecules. Thus, sesquiterpenes from copaiba oil can perform a significant role in the inhibition of these essential macromolecules for viral replication.[36]

Additionally, α-humulene has shown the best docking score with PDB: 6M71 (affinity energy of −6.4 kcal mol⁻¹) (Figure 3e; Table 4) while β-bisabolene was the worst to the same host macromolecule (−4.9 kcal mol⁻¹). Thus, α-humulene interacted with seven hydrophobic residues (Asp218, Asn209, Tyr217, Arg33, Thr123, Phe35, and Lys50) and one hydrogen bond with the Arg 116 at 3.09 Å. APBS solvation screening shows that the molecule's site is very electrostatically negative.

Regarding the SARS-CoV-2 spike receptor (Figure 3f), β-bisabolene registered the lowest energy binding with PDB:6M0J (−6.8 kcal mol⁻¹) in contrast with germacrene D (−5.6 kcal mol⁻¹). This compound held a very narrow energy difference by comparing it with the other copaiba essential oil compounds. The binding mechanism was hydrophobic interactions with Ala413, Met366, Thr434, Glu430, Pro415, Glu435, Ile291, Asn290, and Phe438 at related hACE2 receptor. β-Bisabolene bonded at domain 5 of the hACE2/Spike S complex, containing an active site with a disulfide bond and zinc-binding site. Therefore, it is a significant indication of inhibition, particularly since hACE2 is an important human target for inhibition to avoid engagement with the SARS-CoV-2 viral spike (S) protein.[32,37] APBS solvation results showed β-bisabolene paired with a very electrostatically electronegative site on the surface complex.

The sesquiterpenes are identified from the essential oil leaves of *Croton cajucara* Benth. showed six main
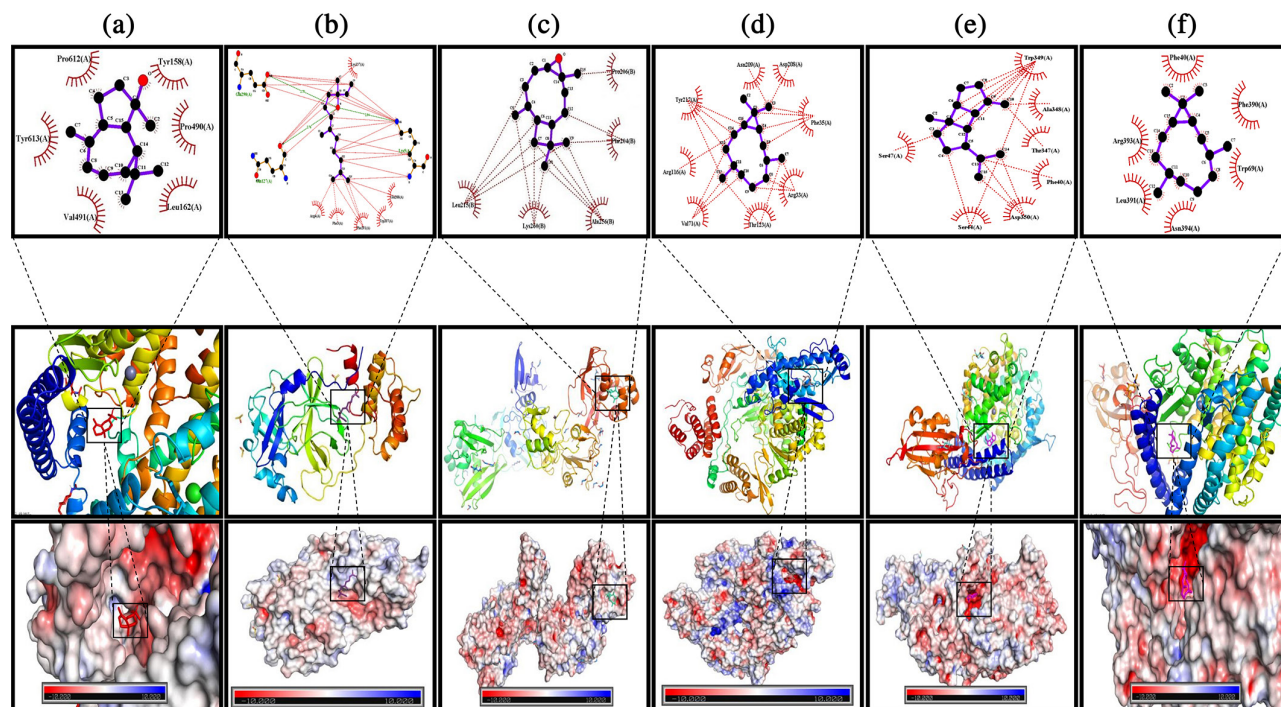
Figure 4. Molecular docking and APBS solvation of *C. cajucara* against the main assayed virus and host domains. (a) Interaction of the ACE 2 with the spathulenol molecule and its APBS solvation; (b) interaction of the SARS-CoV-2 main protease with unliganded active site with the (*E*)-nerolidol molecule and its APBS solvation; (c) interaction of the 1.9 Å crystal structure of NSP15 endoribonuclease from SARS-CoV-2 in the complex with a citrate with the caryophyllene oxide molecule and its APBS solvation; (d) interaction of the SARS-CoV-2 RNA-dependent RNA polymerase in complex with cofactors with the bicyclogermacrene and its APBS solvation; (e) interaction of the crystal structure of SARS-CoV-2 spike receptor-binding domain bound with ACE2 with the β-bisabolene and its APBS solvation; (f) interaction of the crystal structure of SARS-CoV-2 spike receptor-binding domain bound with ACE2 with the bicyclogermacrene and its APBS solvation.

interactions with target SARS-CoV-2 proteins, according to the molecular docking analysis (Figure 4).

Among the analyzed compounds, spathulenol showed the best binding sites and also the highest energy binding levels observed on electrostatic solvation with hACE2. For the other compounds: (*i*) (*E*)-nerolidol the highest energy binding levels were detected with SARS-CoV-2 M-Pro; (*ii*) caryophyllene oxide with SARS-CoV-2 Nsp15/NendoU; (*iii*) bicyclogermacrene with SARS-CoV RdRp; and (*iv*) β-bourbonene and bicyclogermacrene with Spike S macromolecules.

Among *C. cajucara* compounds, spathulenol showed the lowest binding energy (−7.1 kcal mol⁻¹) with ACE2 (PDB: 1R42). Otherwise, the main compound linalool was not satisfactory (−4.9 kcal mol⁻¹). Thus, if compared with all SARS-CoV-2 proteins docked, the best docking scores was obtained from this interaction. Indeed, six spathulenol-PDB:1R42 hydrophobic interactions were found at chain A related to the hACE2 complex (Pro612, Tyr158, Pro490, Leu162, Val491, and Tyr613). Strongest binding determined by APBS was found in a very electronegative site on the electrostatic surface of this complex. Therefore, spathulenol presented a promise inhibitory effect on the hACE2 receptors. From nine

macromolecules related to the SARS-CoV Main Protease, the best energy binding levels was taken to PDB6Y84-(*E*)-nerolidol complex (−7.0 kcal mol⁻¹) (Figure 4b).

Linalool-PDB5R7Z complex showed weak binding affinity (−4.4 kcal mol⁻¹), corroborating with Aanouz *et al.*[38] studies. Meanwhile, (*E*)-nerolidol ligand bound with 6 amino acids on hydrophobic site composed by Lys137, Arg4, Phe3, Phe291, Trp207, and Glu288. There were also three H-bond Glu290, Gln127, and Lys5, with distances of 2.78, 2.76, and 2.94 Å, respectively. This favorable interaction with human hACE2 occurred in the receptor-binding motif (RBM) at the domain 4 sites.[39] The evaluation of the hydrophobic binding residues is as much important as the evaluation of the hydrogen bonds in order to understand the stability of the complex formed.[40] In this way, the presence of hydrogen bond interaction explains a stable interaction between the sesquiterpenes and the studied protein.[38] These bindings happened at the domain I and II of the main proteases.[41] According to Figure 4, it is possible to determine that the sesquiterpenes from *C. cajucara* were binding on the slightly electropositive electrostatic surface.

PDB6W01 was selected between three main SARS-CoV-2 Nsp/NendoU macromolecules sites (Figure 4c). Caryophyllene oxide showed the lowest

binding affinity (−6.9 kcal mol⁻¹), while linalool was the highest (−4.4 kcal mol⁻¹). Caryophyllene oxide ligand bound with 5 amino acids on hydrophobic bonds: Pro206, Phe204, Ala256, Lys260, and Leu215 at the domain II and IV in the chain A of the uridylate-specific endoribonuclease.[42] This molecule linked on a neutral electrostatic site of the molecule, with a slightly negative potential surface. Positive charges are attracted to regions of high electron density (negative potential) and repelled in regions of low electron density (positive potential).[37] Therefore, the studied surface corresponded to a balanced potential density. For the SARS-Cov-2 RNA-dependent RNA polymerase (PDB6M71), the best interaction was observed to the bicyclogermacrene (−6.7 kcal mol⁻¹) (Figure 4d). Linalool showed weak interaction with SARS-Cov-2 protein.[38]

Virtual screening presented potential inhibitions of the protein with most of the molecules through of hydrophobic site composed by Tyr217, Arg116, Val71, Thr123, Arg33, Phe35, Asp208, and Asn209. APBS solvation screening showed that the molecule's site surface is very electronegative, an indication that the molecule of bicyclogermacrene is attracted to this region due to its high electron density. All bindings happened at chain A, which

is related to the NSP-12, corresponding to the domains I, II, and III of the macromolecules.[42]

At last, β-bourbonene and bicyclogermacrene presented the lowest energy binding levels (−6.7 kcal mol⁻¹) with the PDB6M0J, a crystal structure of SARS-CoV-2 Spike S receptor-binding domain bound with hACE2 (Figures 4e and 4f). Hydrophobic interactions were responsible for producing β-bourborene-PDB:6M0J complexes with Ser47, Ser44, Asp350, Phe40, Thr347, Ala348, and Trp349. Bicyclogermacrene-PDB6M0J complexed with Phe40, Phe390, Trp69, Asn394, Leu391, and Arg393. Both interactions were related to the hACE2 domain. The sesquiterpenes were fitted onto the electrostatically electronegative domain on the protein surface corresponding to the domain 1 and 5 receptor-binding site with neither zinc channel.[43] At this position, there is a complete loss of human hACE2 binding *in vitro*.[44] Thus, these sesquiterpenes may inhibit the main host-virus protein complex.

Finally, as the results of the main interactions of *Siparuna guianensis* Aublet. essential oil, five ligand-macromolecule complexes were considered from the molecular docking, according to Figure 5.

The best-docked interaction for sesquiterpenes from *S. guianensis* correspond to: (*i*) γ-eudesmol with hACE2,
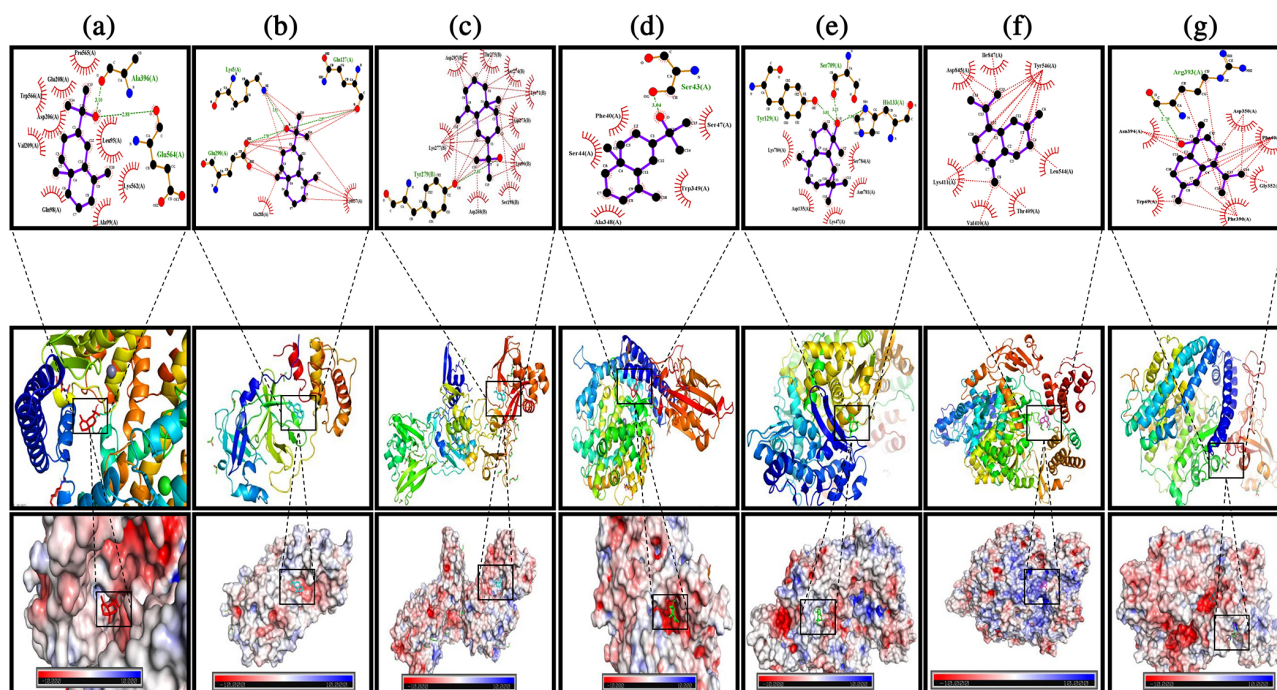

Figure 5. Molecular docking and APBS solvation of *S. guianensis* against the main assayed virus and host domains. (a) Interaction of the ACE 2 with the γ-eudesmol molecule and its APBS solvation; (b) interaction of the SARS-CoV-2 main protease with unliganded active site with the γ-eudesmol molecule and its APBS solvation; (c) interaction of the 1.9 Å crystal structure of NSP15 endoribonuclease from SARS-CoV-2 in the complex with a citrate with the γ-eudesmol molecule and its APBS solvation; (d) interaction of the SARS-Cov-2 RNA-dependent RNA polymerase in complex with cofactors with the α-muurolene and its APBS solvation; (e) interaction of the SARS-Cov-2 RNA-dependent RNA polymerase in complex with cofactors with the spathulenol and its APBS solvation; (f) interaction of the crystal structure of SARS-CoV-2 spike receptor-binding domain bound with ACE2 with the γ-eudesmol and its APBS solvation; (g) interaction of the crystal structure of SARS-CoV-2 spike receptor-binding domain bound with ACE2 with the t-muurolol and its APBS solvation.

SARS-CoV-2 main protease, SARS-CoV-2 Nsp15/NendoU, and SARS-CoV RdRp; (*ii*) spathulenol and γ-eudesmol with SARS-CoV RdRp; and (*iii*) t-muurolol with Spike S macromolecules. As the main result, γ-eudesmol showed the best interaction energy with various macromolecules involved in the SARS-CoV infection (Figures 5a, 5b, 5c, 5d; Table 4). This compound showed the lowest binding affinity to hACE2 (PDB ID 1R42: −7.2 kcal mol^{-1}), SARS-CoV Main Protease (PDB ID 6Y84: −7.5 kcal mol^{-1}), SARS-CoV-2 Nsp15/NendoU (PDB ID 6W01: −7.3 kcal mol^{-1}), and SARS-CoV RdRp (PDB ID 6M71: −6.3 kcal mol^{-1}).

Thus, this promising result indicates the potential application of γ-eudesmol in different ways to prevent or treat the severe acute respiratory infections caused by SARS-CoV-2. The lowest binding energy was related to γ-eudesmol- SARS-CoV Main Protease complex, suggesting this route as the preferable one for treating the viral infection. About hACE2, γ-eudesmol interacted by hydrophobic and hydrogen bonds with the amino acid at a very electronegative site on the electrostatic surface of this complex.[41] The main interaction of the γ-eudesmol with ACE2 occurred in the RBM domain at Zn binding active site, proving an opportunity to uncover a cross-reactive epitope of protein.[45]

In addition, γ-eudesmol also interacted with peptidase M2 at the region responsible for glycosylation reactions, slightly inhibiting interaction with SARS-CoV Spike glycoprotein. In another way, SARS-CoV Main Protease had an excellent virtual screening with γ-eudesmol, showing hydrophobic bonds at the electrostatic site of greater electronegativity of the molecule. SARS-CoV-2 Nsp15/NendoU formed a complex with the sesquiterpene by hydrophobic and strong hydrogen bonds predominantly in the site with an isocontour of the electrostatic potential surface at a sheet of the uridylate-specific endoribonuclease, two domains (I and IV) and a helix.[36]

SARS-Cov-2 RNA-dependent RNA polymerase interacted with γ-eudesmol, spathulenol, and α-muurolene showing the same energy value (PDB6M71 = −6.3 kcal mol^{-1}) (Figures 5d, 5e, 5f). These complexes displayed a lower binding affinity compared with other proteins. The complexes were formed by hydrophobic and hydrogen bonds at a different electrostatic potential surface of the macromolecule (electronegative, neutral, and electropositive for γ-eudesmol, spathulenol, and α-muurolene, respectively). The interaction occurred according to: (*i*) γ-eudesmol: in the domain 1 at Nsp8 interaction site for; (*ii*) spathulenol: in domain 1 as a putative inhibitor binding site and conserved polymerase motif D, and also in domain 3; and (*iii*) α-muurolene:

domain 1 conserving the polymerase motif F and as a putative inhibitor binding site, and also in domain 4 (Nsp7 interaction site).

For the other twelve tested compounds, t-muurolol had the lowest energy binding level interacting with the crystal structure of the SARS-CoV-2 Spike S receptor-binding domain bound with hACE2 (Figure 5g). The weakest energy level (−5.8 kcal mol^{-1}) corresponded to the protein complex formed with elemol and with iso-shyobunone. The sesquiterpene t-muurolol fits by hydrophobic and hydrogen bonds in a very electrostatically electronegative site on the complex surface (Arg393 (2.78 Å), Asp350, Phe40, Gly352, Phe390, Trp69, and Asn394). In addition, this compound was bound at the receptor-binding site in domain 5, which partially inhibits the human hACE2 binding *in vitro*.[32,40]

Conclusions

The present study provided a potential approach to the application of 31 sesquiterpenes identified from the essential oils of *Copaifera langsdorffii* Desf., *Croton cajucara* Benth., and *Siparuna guianensis* Aublet., which were characterized by using GC-MS and GC-FID techniques. These compounds assayed by the molecular docking applying the AutoDock Vina software showed to be promising candidates to further studies against coronavirus (SARS-CoV-2). Indeed, all tested compounds have shown good potential to inhibit both viral proteins and hACE2 protein, blocking the host receptor and also attacking the macromolecules of SARS-CoV-2 M-Pro, SARS-CoV-2 Nsp15/NendoU, SARS-CoV RdRp, and Spike S protein groups, that represent the major proteins of SARS-CoV-2, responsible to originate the disease COVID-19. Molecular docking attested the spontaneous interaction of all investigated compounds with active sites of viral and human proteins, by strongly binding to their amino acids. Analyzing the anchorage simulation, sesquiterpenes showed a high binding affinity with only one or several target proteins at the same time. Therefore, the present study reinforces that natural oils should be considered as candidates to further studies, considering that the SARS-CoV-2 pandemic is not over. Thus, there is a social and scientific utmost need for further *in vitro* and *in vivo* studies focusing on discovering therapeutic adjuvants against SARS-CoV-2 infection.

Acknowledgments

Author Contributions

Rêmullo B. G. M. Costa was responsible for methodology and software analysis; Regildo M. G. Martins for methodology and software analysis; Gerlane S. de Lima for original draft preparation; Thayza C. M. Stamford for methodology and original draft preparation; Wanderli P. Tadei for formal analysis; Maria Aparecida M. Maciel for data curation, writing-reviewing and editing; Amália C. M. do Rêgo for supervision and investigation; Francisco H. Xavier-Júnior for conceptualization, supervision, writing-reviewing and editing.

References

1. Silva, J. K. R.; Figueiredo, P. L. B.; Byler, K. G.; Setzer, W. N.; *Int. J. Mol. Sci.* **2020**, *21*, 3426.

2. Xia, S.; Liu, M.; Wang, C.; Xu, W.; Lan, Q.; Feng, S.; Qi, F.; Bao, L.; Du, L.; Liu, S.; Qin, C.; Sun, F.; Shi, Z.; Zhu, Y.; Jiang, S.; Lu, L.; *Cell Res.* **2020**, *30*, 343.

3. World Health Organization (WHO); *Coronavirus Disease 2019 (COVID-19): Situation Report 151*; https://www.who.int/docs/default-source/coronaviruse/situation-reports/20200619-covid-19-sitrep-151.pdf?sfvrsn=8b23b56e_2, accessed in October 2021.

4. McKee, D. L.; Sternberg, A.; Stange, U.; Laufer, S.; Naujokat, C.; *Pharmacol. Res.* **2020**, *157*, 104859.

5. Thuy, B. T. P.; My, T. T. A.; Hai, N. T. T.; Hieu, L. T.; Hoa, T. T.; Thi Phuong Loan, H.; Triet, N. T.; Anh, T. T. V.; Quy, P. T.; Tat, P. V.; Hue, N. V.; Quang, D. T.; Trung, N. T.; Tung, V. T.; Huynh, L. K.; Nhung, N. T. A.; *ACS Omega* **2020**, *5*, 8312.

6. Morse, J. S.; Lalonde, T.; Xu, S.; Liu, W. R.; *ChemBioChem* **2020**, *21*, 730.

7. Wrapp, D.; Wang, N.; Corbett, K. S.; Goldsmith, J. A.; Hsieh, C.-L.; Abiona, O.; Graham, B. S.; McLellan, J. S.; *Science* **2020**, *367*, 1260.

8. Cecílio, A. B.; Faria, D. B.; Oliveira, P. C.; Caldas, S.; Oliveira, D. A.; Sobral, M. E. G.; Duarte, M. G. R.; Moreira, C. P. S.; Silva, C. G.; Almeida, V. L.; *J. Ethnopharmacol.* **2012**, *141*, 975.

9. de Medeiros, M. L.; Xavier Jr., F. H.; Araújo Filho, I.; Rêgo, A. C. M.; Veiga Jr., V. F.; Maciel, M. A. M. In E*ncyclopedia of Nanoscience and Nanotechnology*, vol. 27, 1ˢᵗ ed.; Nawla, H. S. ed.; American Scientific Publishers: Valencia, USA, 2019.

10. Xavier-Junior, F. H.; Maciuk, A.; Morais, A. R. V.; Alencar, E. N.; Garcia, V. L.; Egito, E. S. T.; Vauthier, C.; *J. Chromatogr. Sci.* **2017**, *55*, 969.

11. Lim, H.; Min, D. S.; Park, H.; Kim, H. P.; *Toxicol. Appl. Pharmacol.* **2018**, *355*, 93.

12. Lin, S.-C.; Ho, C.-T.; Chuo, W.-H.; Li, S.; Wang, T. T.; Lin, C.-C.; *BMC Infect. Dis.* **2017**, *17*, 144.

13. Ryu, Y. B.; Jeong, H. J.; Kim, J. H.; Kim, Y. M.; Park, J.-Y.; Kim, D.; Naguyen, T. T. H.; Park, S.-J.; Chang, J. S.; Park, K. H.; *Bioorg. Med. Chem.* **2010**, *18*, 7940.

14. Lopes, D.; Blzzo, H. R.; Sá Sobrinho, A. F.; Pereira, M. V. G.; *J. Essent. Oil Res.* **2000**, *12*, 705.

15. Aguiar, R. W. S.; Santos, S. F.; Morgado, F. S.; Ascencio, S. D.; Lopes, M. M.; Viana, K. F.; Didonet, J.; Ribeiro, B. M.; *Plos One* **2015**, *10*, e0116765.

16. Valentini, C. M. A.; da Silva, L. E.; Maciel, E. N.; Franceschini, E.; Sousa Jr., P. T.; Dall'Oglio, E. L.; Coelho, M. F. B.; *Quim. Nova* **2010**, *33*, 1506.

17. Kim, S.; Chen, J.; Cheng, T.; Gindulyte, A.; He, J.; He, S.; Li, Q.; Shoemaker, B. A.; Thiessen, P. A.; Yu, B.; Zaslavsky, L.; Zhang, J.; Bolton, E. E.; *Nucleic Acids Res.* **2021**, *49*, D1388.

18. O'Boyle, N. M.; Banck, M.; James, C. A.; Morley, C.; Vandermeersch, T.; Hutchison, G. R.; *J. Cheminf.* **2011**, *3*, 33.

19. Morris, G. M.; Huey, R.; Lindstrom, W.; Sanner, M. F.; Belew, R. K.; Goodsell, D. S.; Olson, A. J.; *J. Comput. Chem.* **2009**, *30*, 2785.

20. Waterhouse, A.; Bertoni, M.; Bienert, S.; Studer, G.; Tauriello, G.; Gumienny, R.; Heer, F. T.; Beer, T. A. P.; Rempfer, C.; Bordoli, L.; Lepore, R.; Schwede, T.; *Nucleic Acids Res.* **2018**, *46*, W296.

21. Grosdidier, A.; Zoete, V.; Michielin, O.; *Nucleic Acids Res.* **2011**, *39*, W270.

22. Grosdidier, A.; Zoete, V.; Michielin, O.; *J. Comput. Chem.* **2011**, *32*, 2149.

23. Berman, H. M.; *Nucleic Acids Res.* **2000**, *28*, 235.

24. Trott, O.; Olson, A. J. A. V.; *J. Comput. Chem.* **2010**, *31*, 455.

25. Costa, R. B. G. M.; *DockME LITE® v.1.0.5 Alpha*; RB aresta, Brazil, 2020.

26. *PyMOL*, v. 2.0; DeLano Scientific, USA, 2017.

27. Laskowski, R. A.; Swindells, M. B.; *J. Chem. Inf. Model.* **2011**, *51*, 2778.

28. Gramosa, N. V.; Silveira, E. R.; *J. Essent. Oil Res.* **2005**, *17*, 130.

29. Soares, D. C.; Portella, N. A.; Ramos, M. F. S.; Siani, A. C.; Saraiva, E. M.; *J. Evidence-Based Complementary Altern. Med.* **2013**, *2013*, ID 761323.

30. Lemos, T. L. G.; Machado, M. I. I.; Menezes, J. E. S. A.; Sousa, C. R.; *J. Essent. Oil Res.* **1999**, *11*, 411.

31. Azevedo, M.; Chaves, F.; Almeida, C.; Bizzo, H.; Duarte, R.; Campos-Takaki, G.; Alviano, C.; Alviano, D.; *Molecules* **2013**, *18*, 1128.

32. Das, S.; Sarmah, S.; Lyndem, S.; Singha Roy, A.; *J. Biomol. Struct. Dyn.* **2021**, *39*, 3347.

33. Shah, B.; Modi, P.; Sagar, S. R.; *Life Sci.* **2020**, *252*, 117652.

34. Jin, Z.; Du, X.; Xu, Y.; Deng, Y.; Liu, M.; Zhao, Y.; Zhang, B.; Li, X.; Zhang, L.; Peng, C.; Duan, Y.; Yu, J.; Wang, L.; Yang, K.; Liu, F.; Jiang, R.; Yang, X.; You, T.; Liu, X.; Yang, X.; Bai, F.; Liu, H.; Liu, X.; Guddat, L. W.; Xu, W.; Xiao, G.; Qin, C.; Shi, Z.; Jiang, H.; Rao, Z.; Yang, H.; *Nature* **2020**, *582*, 289.

35. Michalska, K.; Quan Nhan, D.; Willett, J. L. E.; Stols, L. M.; Eschenfeldt, W. H.; Jones, A. M.; Nguyen, J. Y.; Koskiniemi, S.; Low, D. A.; Goulding, C. W.; Joachimiak, A.; Hayes, C. S.; *Mol. Microbiol.* **2018**, *109*, 509.

36. Kim, Y.; Jedrzejczak, R.; Maltseva, N. I.; Wilamowski, M.; Endres, M.; Godzik, A.; Michalska, K.; Joachimiak, A.; *Protein Sci.* **2020**, *29*, 1596.

37. Babcock, G. J.; Esshaki, D. J.; Thomas, W. D.; Ambrosino, D. M.; *J. Virol.* **2004**, *78*, 4552.

38. Aanouz, I.; Belhassan, A.; El-Khatabi, K.; Lakhlifi, T.; El-ldrissi, M.; Bouachrine, M.; *J. Biomol. Struct. Dyn.* **2021**, *39*, 2974.

39. Wan, Y.; Shang, J.; Graham, R.; Baric, R. S.; Li, F.; *J. Virol.* **2020**, *94*, e00127-20.

40. Kumar, A.; Choudhir, G.; Shukla, S. K.; Sharma, M.; Tyagi, P.; Bhushan, A.; Rathore, M.; *J. Biomol. Struct. Dyn.* **2021**, *39*, 3760.

41. Zhang, L.; Lin, D.; Sun, X.; Curth, U.; Drosten, C.; Sauerhering, L.; Becker, S.; Rox, K.; Hilgenfeld, R.; *Science* **2020**, *368*, 409.

42. Carey, F. A.; Sundberg, R. J.; *Advanced Organic Chemistry*, 5th ed.; Springer: New York, 2007.

43. Zheng, B.-J.; Guan, Y.; Hez, M.-L.; Sun, H.; Du, L.; Zheng, Y.; Wong, K.-L.; Chen, H.; Chen, Y.; Lu, L.; Tanner, J. A.; Watt, R. M.; Niccolai, N.; Bernini, A.; Spiga, O.; Woo, P. C. Y.; Kung, H.; Yuen, K.-Y.; Huang, J.-D.; *Antiviral Ther.* **2005**, *10*, 393.

44. Wong, S. K.; Li, W.; Moore, M. J.; Choe, H.; Farzan, M.; *J. Biol. Chem.* **2004**, *279*, 3197.

45. Yuan, M.; Wu, N. C.; Zhu, X.; Lee, C.-C. D.; So, R. T. Y.; Lv, H.; Mok, C. K. P.; Wilson, I. A.; *Science* **2020**, *368*, 630.